

# Photovoltaic spectra and magneto-optical transitions in InSb

P. Rochon and E. Fortin

*Department of Physics, University of Ottawa, Ottawa, Canada*

(Received 27 October 1976)

Spectral oscillations are observed in the photoresponse of a gold-indium-antimonide Schottky barrier in magnetic fields of up to 3 Tesla. The photovoltaic spectra are taken at 6 K in the Faraday configuration with  $\vec{B}$  parallel to [111]. Both exciton and Landau spectral structures are observed and separately analyzed: the Landau levels in terms of the Pidgeon and Brown coupled-bands theory and the exciton states in terms of the adiabatic theory recently proposed by Altarelli and Lipari. In both analyses, the parameters of Pidgeon and Brown for InSb are found to give the best fit to the magneto-optical data. The behavior in the magnetic field of a structure arising from transitions between an acceptor state at 2.8 meV above the valence band to the conduction band is also observed and analyzed.

## I. INTRODUCTION

In recent years, a great deal of theoretical and experimental effort has been expended in order to understand the electronic states which give rise to the structures observed in interband magneto-optical spectra and their relation to the band parameters of semiconductors. The theory for the quantization of electronic levels in a magnetic field was first developed by Landau.<sup>1,2</sup> It was later refined by Luttinger and Kohn<sup>3</sup> to include the valence-band degeneracy occurring in many real semiconductors and further refined by Pidgeon and Brown<sup>4</sup> to include the nonparabolicity of the conduction band. However, in interband magneto-optics, one can use the above theories directly only in cases where excitonic contributions to the spectra can be either neglected or at least separated from the continuum. The behavior of exciton states in a magnetic field can be studied following the theories developed by Elliott and Loudon<sup>5</sup> and, more recently, by Altarelli and Lipari.<sup>6,7</sup> The problem of the exciton in a magnetic field has been solved completely only for the cases of low and high fields (i.e.,  $\gamma \ll 1$  and  $\gamma \gg 1$ , where  $\gamma = \hbar\omega_c/2R_0$ , the ratio of the cyclotron energy to the exciton binding energy).

Indium antimonide was one of the first semiconductors studied in magneto-optics because its low conduction-band effective mass permitted the observation of well-defined magneto-optical structures at moderately high magnetic fields. For InSb,  $\gamma = 1$  at  $B = 0.11$  T, so that the recent theory of Altarelli and Lipari<sup>7</sup> for the behavior of excitons in high fields ( $\gamma \gg 1$ ) can be applied. In fact, for InSb, a separate analysis of the exciton states' behavior in a magnetic field and of the Landau levels can now be done and, as a result, the band parameters which best fit both phenomena simultaneously can be determined.

The study of photovoltaic spectra has recently proved to be a successful method for collecting interband magneto-optical data in semiconductors.<sup>8,9</sup> The advantages of the method over usual absorption and reflectivity techniques include a high signal-to-noise ratio and experimental simplicity, since there is no need for thin samples or external detectors. In addition, the photovoltaic sample can be made to reflect small changes in the absorption coefficient with a high degree of sensitivity.

In the following paragraphs, a brief review of the theories on the effects involved and used here is presented, followed by a description of the experimental set-up and a discussion of the magneto-optical results obtained from photovoltaic spectra on Au-InSb Schottky barriers. The data corresponding to Landau levels are analyzed in terms of the Pidgeon and Brown<sup>4</sup> theory, and the exciton states' behavior is analyzed separately in terms of the theory by Altarelli and Lipari.<sup>7</sup> A spectral structure associated with impurity absorption is also observed, and its behavior in the magnetic field is analyzed as well.

## II. THEORETICAL BACKGROUND

### A. Photovoltaic effect

The open-circuit zero-bias photovoltage  $V_{pv}$  across an illuminated Schottky barrier can be shown to be<sup>10</sup>

$$V_{pv} = (kT/e) \ln(1 - J/J_s) \quad , \quad (1)$$

where  $J_s$  is the reverse-bias-saturation current density, and  $J$  is the nonequilibrium current density resulting from the illumination. In the case of a metal-*n*-type semiconductor junction, the photocurrent is given by<sup>12</sup>

$$J = -q\phi [1 - e^{-\alpha W} / (1 + \alpha L_p)] \quad , \quad (2)$$

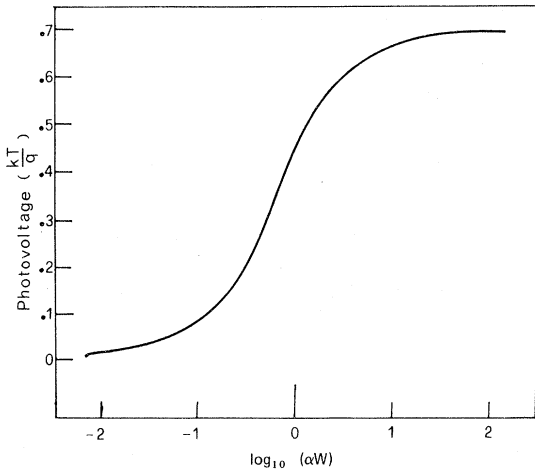


FIG. 1. Photovoltage as a function of  $\log_{10}(\alpha W)$  for values of  $\alpha L_p \ll 1$  and  $q\phi/J_s = 1$ . For a fixed depletion width  $W$ , the photovoltage is insensitive to changes in the absorption coefficient  $\alpha$  for  $\alpha W < 10^{-1}$  and  $\alpha W > 10$ . The highest sensitivity to small changes in  $\alpha$  occurs at  $\alpha W \approx 1$ .

where  $\phi$  is the incident photon flux times the quantum efficiency,  $\alpha$  is the absorption coefficient of the semiconductor,  $L_p$  is the hole diffusion length, and  $W$  is the barrier depletion width which in the abrupt junction approximation is expressed as<sup>10</sup>

$$W = (2\epsilon_s \phi_B / qN_d)^{1/2}. \quad (3)$$

Here  $\epsilon_s$  is the effective permittivity of the semiconductor,  $\phi_B$  is the barrier height, and  $N_d$  is the density of ionized donors. The sensitivity of the photovoltage to small changes in the absorption coefficient is mainly determined by the value of  $W$ : this is illustrated in Fig. 1 where the behavior of the photovoltage as a function of  $\log_{10}(\alpha W)$  has been calculated following Eqs. (1) and (2). The photovoltage is insensitive to small changes in the absorption coefficient  $\alpha$  for  $\alpha W < 10^{-1}$  and  $\alpha W > 10$ , and is most sensitive in the region near  $\alpha W = 1$ . The barrier width in turn is determined by  $N_d$  and  $\phi_B$  [Eq. (3)]; therefore, a selection of the proper donor concentration and of the metallic barrier can result in samples most suitable for the observation of small changes in  $\alpha$ , and, in particular, of magneto-optical structures.

#### B. Magneto-optics

In the proper circumstances, the spectral distribution of the photovoltaic effect will thus display structures related to interband magneto-optical transitions which are usually observed in absorption or reflectivity spectra. Analysis of the structures with the help of appropriate theories will in turn allow a precise determination of the band parameters of the semiconductor. The Pidgeon and

Brown<sup>4</sup> theory for interband magneto-optical transitions is, to date, the most realistic theory for the displacement of Landau-level-associated transitions, as a function of magnetic field. The theory takes into account the valence-band degeneracy as well as the interaction between the valence bands, conduction band, and the upper bands.

The experimental results, however, include contributions not only from Landau-like transitions but also reflect the participation of excitons associated with each Landau level. Elliott and Loudon<sup>5</sup> demonstrated that exciton states, in the presence of high magnetic fields, can be associated with each Landau magnetic sublevel and that these states can be expected, in some cases, to be the dominating features in the spectra. When the magnetic field can be made high enough ( $\gamma \gg 1$ , as in the case for InSb) it is possible to identify the structures belonging to exciton states separately from those associated with Landau levels. The behavior of the exciton states in the magnetic field can then be independently fitted to the theory of Altarelli and Lipari<sup>7</sup> which is valid for  $\gamma \gg 1$ , and in contrast to previous theories, takes into account the valence-band degeneracy and anisotropy, as well as band-to-band interactions (non-parabolicity). From the analysis of magneto-optical spectra in InSb, it should therefore be possible to obtain a set of band parameters which are consistent with both types of magneto-optical phenomena.

#### III. EXPERIMENTAL

The samples are cut from a monocrystalline block of  $n$ -type InSb with a room-temperature carrier concentration of  $10^{16} \text{ cm}^{-3}$ . This material is pure enough to obey the condition  $\omega\tau > 1$  required for the observation of well-defined magneto-optical structures (at 6 K, an experimental value of  $\omega\tau = 5$  is obtained). At the same time, the impurity concentration should be high enough to satisfy the barrier width condition, as well as provide a moderate electric field at the junction. The samples fulfill the above conditions, since quantum oscillations were indeed observed while, at the same time, no Franz-Keldish effects were detected at 6 K. In fact, a rough estimate with<sup>13</sup>  $\epsilon_s = 16.8$  and  $\phi_B = 0.18 \text{ eV}$  gives the barrier width  $W \approx 2 \times 10^{-5} \text{ cm}$  with a maximum electric field of  $E \approx 10^4 \text{ V/cm}$  at the barrier.

The samples were polished with  $\text{Al}_2\text{O}_3$  powder, etched in a solution of  $\text{HNO}_3$ , and kept in an inert atmosphere or high vacuum during the remainder of the preparation in order to minimize surface oxidation and the resultant changes in the spectra.<sup>11</sup> The contacts on the photovoltaic samples were placed in a "sandwich" configuration, the back

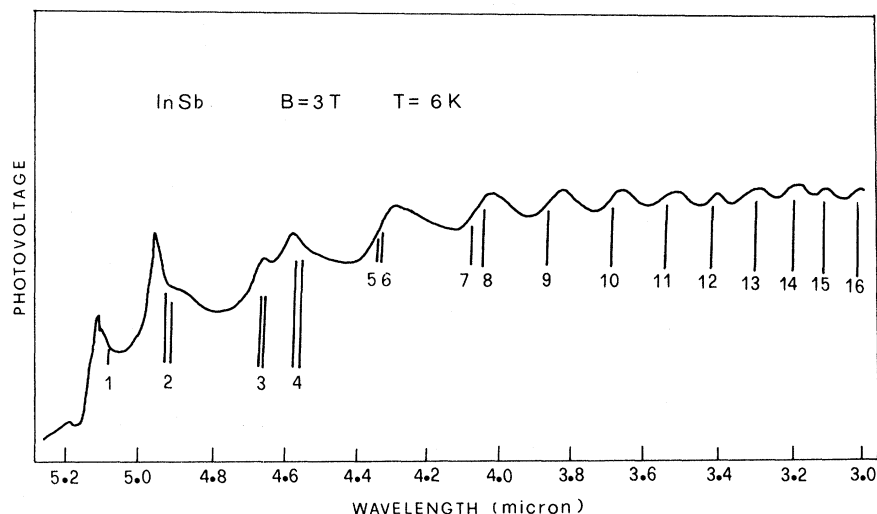


FIG. 2. Spectral distribution of the photovoltage in InSb at a magnetic field of 3 T. The indicated transitions are those associated with Landau levels and are labeled as in Table II.

contact being made of evaporated indium subsequently alloyed in a nitrogen atmosphere furnace at 300°C, and the front contact consisting of an evaporated semitransparent gold film. The samples were mounted in the Faraday configuration in such a manner that  $\vec{S} \parallel \vec{B} \parallel \vec{E} \parallel [111]$ , where  $\vec{S}$  is the incident-radiation propagation vector,  $\vec{B}$  is the magnetic field, and  $\vec{E}$  is the junction electric field. The samples were placed in an independent chamber within a superconducting magnet and kept at 6 K by a He exchange gas at a pressure of 1 kPa. The chamber cold window was made of sapphire while the outer room-temperature window of the cryostat was of  $\text{CaF}_2$ .

The optical system consisted of a  $\frac{3}{4}$ -m grating monochromator mounted in a double-beam geometry, with a second Au-InSb detector in a liquid- $\text{N}_2$  optical cryostat serving as a monitor of the incident-radiation intensity. The photosignals were processed by standard synchronous detection and electronic division techniques.

#### IV. RESULTS AND ANALYSIS

##### A. Landau-level analysis

A typical spectrum of the photoresponse in InSb in the presence of a magnetic field is presented in Fig. 2. The figure is a reduced version of the

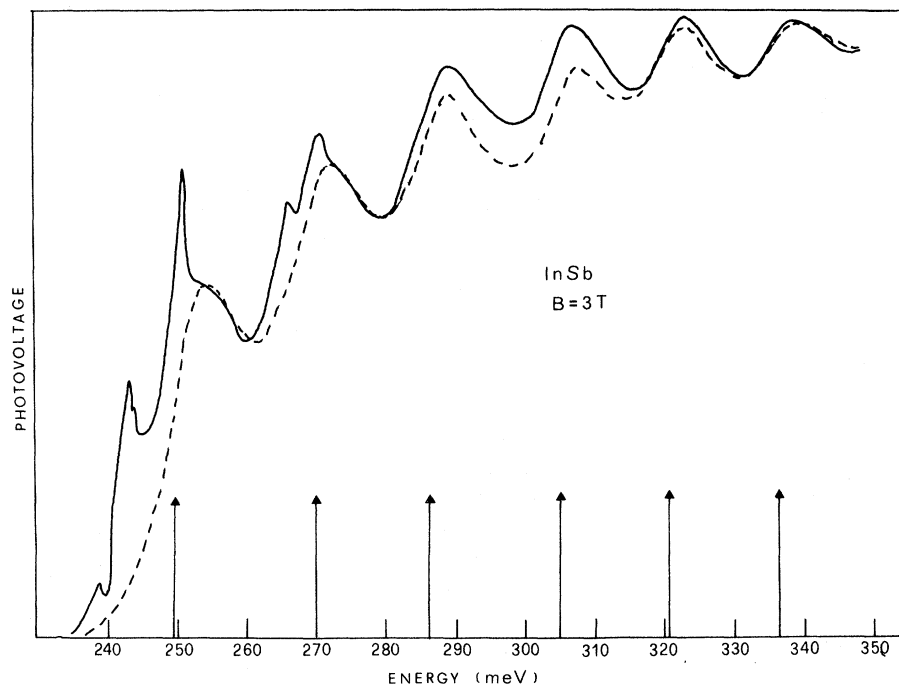


FIG. 3. Comparison between the experimental photoresponse and the calculated photoresponse. The positions of the Landau-level associated transitions are indicated by the arrows; the dashed line is the calculated photoresponse expected for the above Landau levels including a broadening factor ( $\omega\tau=5$ ). The full line is the observed spectral distribution of the photovoltage clearly showing the pronounced exciton participation at low energies. The energy positions of the Landau levels correspond closely to the positions of maximum slope of the high-energy structures.

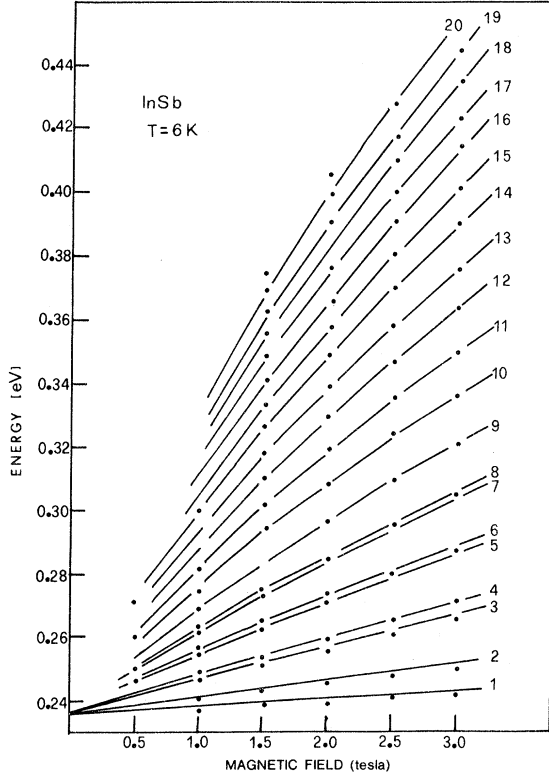


FIG. 4. Energy positions of the maximum slope of the spectral oscillations observed in the photoresponse as functions of the magnetic field. The full lines are the calculated transitions using the parameters of Pidgeon and Brown (Ref. 4) and are labeled according to Table II.

actual spectrum. Photovoltaic spectra of this type were obtained at every 0.5 T in the range 0–3 T and in the wavelength range of 380–540 nm. The structures at high energies were first assumed to

originate from transitions between Landau levels because of both their shape and energy positions. In Fig. 3, we show a graph of the expected spectrum for Landau levels together with the actual spectrum. The theoretical spectrum was obtained by using Eq. (1) for the photovoltage along with the expression for the absorption coefficient as given by Roth *et al.*<sup>14</sup> for the case of Landau-like transitions

$$\alpha(\omega) = \frac{A\omega_c^*}{2\omega} \sqrt{\tau} \sum_{n=1}^{\infty} \left( \frac{(X_n^2 + 1)^{1/2} + X_n}{2(X_n^2 + 1)} \right)^{1/2}, \quad (4)$$

where  $X_n = (\omega - \omega_n)\tau$ ,  $\omega$  is the incident photon frequency,  $\omega_n = \omega_g + (n + \frac{1}{2})\omega_c^*$ , and  $\omega_c^*$  is the effective cyclotron frequency:  $\omega_c^* = eB/\mu$ . The calculated spectrum fitted best the experimental spectrum for  $\omega_c^*\tau = 5$ . It can be seen that for energies greater than 280 meV the structures in the experimental photovoltaic spectrum correspond closely to the calculated Landau-like transitions and that the pertinent positions for the transitions are the energy values of the maximum slope on the low-energy side of the structures. These energies were taken as data and are plotted as functions of the magnetic field in Fig. 4. By extrapolating the values of the points corresponding to Landau-level transitions to zero magnetic field, the band-gap value was found to be  $E_g = 235.5$  meV in agreement with Zwerdling *et al.*'s<sup>15</sup> value of 235.7 meV. The data of the lines 9–19 were considered as Landau levels and using Pidgeon and Brown's coupled-band theory, were compared to the theoretical lines predicted by various sets of parameters for InSb found in the literature (Table I). The parameters of Pidgeon and Brown<sup>4</sup> gave the best fit to the data and the theoretical lines indicated in Figs. 2 and 4 are those obtained by this fit and are labeled in

TABLE I. Band parameters of indium antimonide as given by various authors. The parameters of Pidgeon and Brown (Ref. 4) gave the best fit to the present magneto-optical data.

Parameter	Source				
	a	b	c	d	e
$m_c/m_0$	0.0145	0.0145	0.0145	...	0.014
$g_c$	-48	-48	-48	...	-48.4
$\gamma_1^L$	32.5	33.5	36.0	25	35.08
$\gamma_2^L$	14.3	14.5	14.5	10.5	15.64
$\gamma_3^L$	15.4	15.7	16.2	11.5	16.91
$K^L$	13.4	13.5			14.76
$q^L$	0.4	0.4			0.15

<sup>a</sup>Pidgeon and Brown (Ref. 4).

<sup>b</sup>Pidgeon and Groves (Ref. 16).

<sup>c</sup>Zwerdling *et al.* (Ref. 15).

<sup>d</sup>Bagguley *et al.* (Ref. 17).

<sup>e</sup>Lawaetz theory (Ref. 18).

TABLE II. Identification of the transitions in InSb [in the Pidgeon and Brown (Ref. 4) notation].

No.	HH( <i>n</i> ): $\frac{1}{2}[a^-(n+1)a^c(n) + b^-(n-1)b^c(n)]$	No.	Transition
1	$a^-(1)a^c(0)$	11	HH(6)
2	$b^-(1)b^c(0); b^+(-1)b^c(0)$	12	HH(7)
3	$a^+(1)a^c(0); a^-(2)a^c(1)$	13	HH(8)
4	$b^+(0)b^c(1); b^-(2)b^c(1)$	14	HH(9)
5	$a^-(3)a^c(2)$	15	HH(10)
6	$b^-(1)b^c(2)$	16	HH(11)
7	$a^-(4)a^c(3)$	17	HH(12)
8	$b^-(4)b^c(3); b^-(2)b^c(3)$	18	HH(13)
9	HH(4)	19	HH(14)
10	HH(5)	20	HH(15)

Table II. Although the data for Landau levels of high quantum number were very well fitted, the lower-energy structures differed in both their shape and position from the structures expected for Landau levels as can clearly be seen on Fig. 3.

#### B. Exciton analysis

An expanded spectrum of the photovoltage in the energy region near the fundamental gap is presented in Fig. 5. Except for the impurity absorption peak (*I*) below the gap, the zero-magnetic-field spectrum has no evident structure. The exciton is not resolved in this spectrum because of its low binding energy ( $R_0 = 0.45$  meV). The photoresponse in a high magnetic field, where  $\gamma \gg 1$ , for example at 3 T in the above figure, does show well-defined peaks (*A, B, C*). These structures differ from the expected Landau-level peaks in

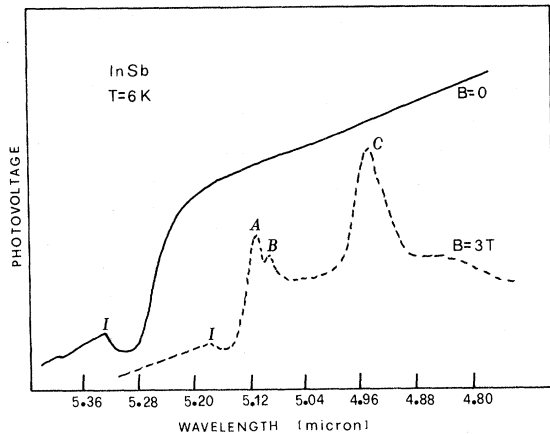


FIG. 5. Expanded  $V_{pv}$  spectrum for energies near the fundamental edge. The structure *I* is associated with a transition from an impurity level. The structures *A, B* and *C* correspond to exciton states; they are labeled in Table III and plotted as functions of the magnetic field in Fig. 6.

both their lineshape (they are strong and sharp), and their positions (they are below the expected energy positions). The structures were then interpreted as originating from exciton states associated with the lower Landau-level edges. The peaks were observed at various magnetic fields and the energy positions of the maxima are plotted as functions of the field in Fig. 5. Using the various sets of band parameters (Table I) the theoretical energies for exciton states in the magnetic field were computed following the theory of Altarelli and Lipari<sup>7</sup> using the Hamiltonian matrix for  $\vec{B} \parallel [111]$  which we have developed.<sup>19</sup> As in the case of the Landau-level analysis, the parameters of Pidgeon and Brown<sup>4</sup> again gave the best fit to the data and the predicted positions are represented in Fig. 6 by the solid lines. These theoretical lines correspond to exciton states associated with the Landau-level labeled  $b^+(1)b^c(0)$  and are labeled in the Altarelli and Lipari formalism as ( $A \rightarrow l=0, n=-3$ , spin up;  $C \rightarrow l=0, n=-3$ , spin down) (Table III). The structure *B* has not yet been identified. The structure *I* was identified as a transi-

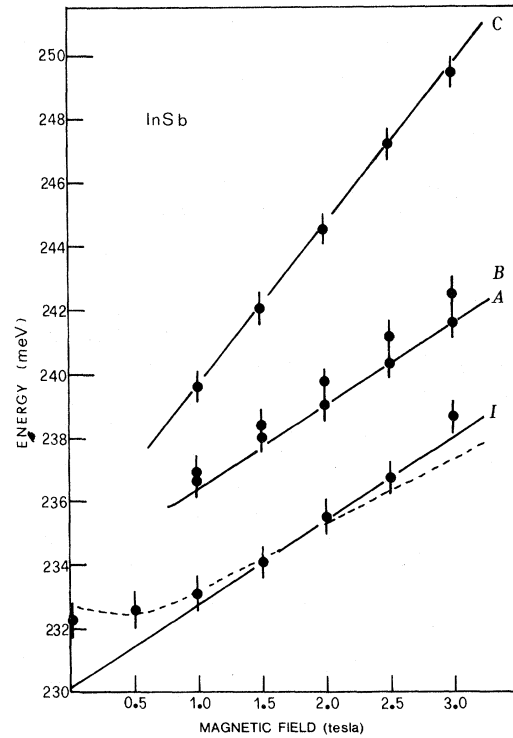


FIG. 6. Energy positions of the structures observed in the photoresponse near the fundamental edge as functions of the magnetic field. The full lines *A* and *C* are the theoretical positions predicted by the theory of Altarelli and Lipari (Ref. 7) for exciton states. The line *I* is the theoretical position of an acceptor level to conduction-band transition with (dashed line) and without (full line) Coulomb interaction.

TABLE III. Identification of transitions in InSb. Exciton states, following the notation of Altarelli and Lipari (Ref. 7).

Peak No.	Spin	$L$	$n$	Corresponding Landau edge
A	up	0	-3	$b^*(1)b^c(0)$
C	down	0	-3	$b^*(1)b^c(0)$

tion originating from an acceptor impurity of the type reported by Johnson and Fan.<sup>20</sup>

### C. Impurity structure

The theory for the behavior of impurity transitions in a magnetic field has been reviewed by Johnson.<sup>14</sup> Structures corresponding to these impurity transitions should occur at a photon energy

$$h\nu = E_g - E_A + \epsilon_c(H) + \epsilon_A(H), \quad (5)$$

where  $E_A$  is the acceptor ionization energy in the absence of magnetic field,  $\epsilon_c(H)$  is the shift of the lowest Landau level ( $n=0$ ) of the conduction band, and  $\epsilon_A(H)$  is the shift of the impurity levels in a magnetic field. For low-magnetic-field values, when  $\epsilon_c(H) \ll E_g$ , the shift of the lowest Landau levels of the conduction band can be expressed as

$$\epsilon_c(H) \simeq \left( \frac{m}{m_c} \pm \frac{1}{2} g_c \right) \mu_B \left| 1 - \left( \frac{m}{m_c} \pm g_c \right) \frac{\mu_B}{E_g} \right|, \quad (6)$$

where  $\mu_B$  is the Bohr magneton.

The magnetic-field-induced energy shift of the acceptor state  $\epsilon_A(H)$  includes both the Zeeman splitting and the diamagnetic shift; but because of the high effective mass of the state, the contribution of  $\epsilon_A(H)$  should be small and will be neglected. The theoretical solid line *I* in Fig. 6 was computed using Eqs. (5) and (6) with  $m_c = 0.0145m_0$ ,  $g_c = -48$ , and  $E_g = 235.5$  meV (Table I). The fit predicts an extrapolated acceptor ionization energy of 5.4 meV.

It has been assumed in the above calculation that the structure observed is due to a free state of the electron in the conduction band. The curvature of the points at low magnetic field, however, suggests that Coulomb interaction between the hole in the acceptor state and the electron in the conduction band should not be neglected, and that the structure *I* corresponds to a bound state of the elec-

tron-hole pair. In this case the photon energy at which absorption occurs is written

$$h\nu = E_g + \epsilon_c - R(H) - E_A, \quad (7)$$

where  $R(H)$ , the exciton binding energy as a function of magnetic field, was estimated following the calculations by Yafet<sup>21</sup> with  $R_0 = 0.45$  meV. Using Eq. (7) the acceptor ionization energy which fits the data is calculated to be  $E_A = 2.8$  meV, a value identical to that reported by Vinogradova *et al.*<sup>22</sup> The theoretical line predicted by Eq. 7 is represented in Fig. 6 by the dashed line.

### V. CONCLUSION

The band parameters proposed by Pidgeon and Brown for InSb were seen to give the best fit to both the Landau-level behavior and the exciton states' behavior in a magnetic field, as analyzed using the latest available magneto-optical theories. With these parameters most of the structures observed in the spectra can be clearly identified. On the other hand, as previously pointed out, peak *B* of Figs. 5 and 6 has yet to be explained and should be the subject of further investigation.

The observation with relative experimental ease of excellent quality magneto-optical structures as well as of an impurity peak demonstrate the power of the photovoltaic effect as a method of detecting small changes in the absorption coefficient of semiconductors. A much greater sensitivity will in fact be achieved in forthcoming experiments by coupling the photovoltaic method with modulation techniques such as wavelength modulation. It should then be possible to study accurately with this relatively simple method a large variety of optical spectra in semiconductors.

### ACKNOWLEDGMENTS

Professor M. Altarelli (University of Illinois, at Urbana-Champaign) assisted in this work by making available the computer program to calculate the energy positions of the exciton states in a magnetic field. The authors are also indebted to Professor J. C. Woolley and Dr. R. C. Smith for helpful discussions during this work. This research was supported by the National Research Council of Canada.

<sup>1</sup>L. D. Landau, Z. Phys. **64**, 629 (1930).

<sup>2</sup>B. Lax and J. G. Mavroides, in *Semiconductors and Semimetals*, edited by R. K. Willardson and A. C. Beer (Academic, New York, 1972), Vol. 3, p. 326.

<sup>3</sup>J. M. Luttinger and W. Kohn, Phys. Rev. **97**, 869 (1965).

<sup>4</sup>C. R. Pidgeon and R. N. Brown, Phys. Rev. **146**, 575 (1966).

<sup>5</sup>R. J. Elliott and R. Loudon, J. Phys. Chem. Solids **15**, 196 (1960).

<sup>6</sup>M. Altarelli and N. O. Lipari, Phys. Rev. B **7**, 3798 (1973).

<sup>7</sup>M. Altarelli and N. O. Lipari, Phys. Rev. B **9**, 1733 (1974).

<sup>8</sup>P. Rochon and E. Fortin, Can. J. Phys. **52**, 1173 (1974).

<sup>9</sup>P. Rochon and E. Fortin, Phys. Rev. B **12**, 5803 (1975).

- <sup>10</sup>S. M. Sze, *Physics of Semiconductor Devices* (Wiley, New York, 1969), p. 363.
- <sup>11</sup>A. Barbarie and E. Fortin, *J. Phys. Chem. Solids* **35**, 1521 (1974).
- <sup>12</sup>W. N. Gartner, *Phys. Rev.* **116**, 84 (1954).
- <sup>13</sup>C. A. Mead and W. G. Spitzer, *Phys. Rev.* **134**, A173 (1964).
- <sup>14</sup>For example, see *Semiconductors and Semimetals*, edited by R. K. Willardson and A. C. Beer (Academic, New York, 1967), Vol. 3.
- <sup>15</sup>S. Zwerdling, W. H. Kleiner, and J. P. Theriault, *J. Appl. Phys. Suppl.* **32**, 2118 (1961).
- <sup>16</sup>C. R. Pidgeon and S. H. Groves, *Phys. Rev.* **186**, 824 (1969).
- <sup>17</sup>D. M. S. Bagguley, M. L. A. Robinson, and R. A. Stradling, *Phys. Lett.* **6**, 143 (1963).
- <sup>18</sup>P. Lawaetz, *Phys. Rev.* **133**, 439 (1971).
- <sup>19</sup>P. Rochon, Ph.D. thesis (University of Ottawa, 1976) (unpublished).
- <sup>20</sup>E. J. Johnson and H. Y. Fan, *Phys. Rev.* **139**, A1991 (1965).
- <sup>21</sup>Y. Yafet, R. Keyes, and E. N. Adams, *J. Phys. Chem. Solids*, **1**, 137 (1956).
- <sup>22</sup>K. I. Vinogradova, *Acad. Sci. USSR Bull. Phys. Ser.* **28**, 863 (1964).